Želimir Kurtanjek

Causal AI Modelling of Chemical Manufacturing Plants

University of Zagreb, Faculty of Food Technology and Biotechnology, Pierottijeva 6, 10 000 Zagreb, Croatia,
retired, zelimir.kurtanjek@gmail.com

Abstract

The concept of "Industry 5.0" is driving significant changes in the production of chemical products and energy, promoting a shift towards a decarbonized and circular economy. Digitalization, robotics, communications, and artificial intelligence (AI) play crucial roles in fostering the development of necessary technological innovations and enhancing intelligent process control. The application of machine deep learning (ML) yields robust, field-neutral solutions for regression prediction objectives, but it is limited in its capacity to address innovative questions that involve causation and counterfactual analysis. This paper presents a proposed application of Bayesian networks (BN) for structural causal modeling (SCM) in the context of manufacturing plants. A critical feature of SCM modeling is its capacity to integrate extensive prior structural knowledge derived from fundamental chemical engineering principles with structures inferred from experimental data obtained from manufacturing plants. The acquired SCM facilitates the forecasting of causal relationships, the simulation of intervention strategies, and the generation of counterfactual responses essential for process innovations and intelligent process management. The SCM model is presented as a tool for examining causality and control in the intricate Tennessee-Eastman process.

***Keywords**: Bayes network, causality, DAG, ATE, Markov blanket, Tennessee-Eastman-Process*

1. Introduction

As a discipline of computer science, artificial intelligence (AI) has far-reaching effects on all dimensions of industrial process engineering. It is the key aspect of EU Industry 5.0 policy of providing solutions to social challenges by its impact on industry digitalization and robotics, energy production and management, decarbonization, waste management, circular economy, sustainability, and global green transition [1]. The field of process control in chemical manufacturing is emerging as a promising area of research. The American Institute of Chemical Engineering (AIChE) recognizes the significant impact of AI in chemical engineering research and industry. AIChE highlights that AI, particularly machine learning, is being widely embraced to solve complex problems, accelerate research, and enable computations that were previously impossible1. AI is seen as a powerful tool in applications requiring heavy, iterative computing and large data analysis [2]. AIChE also acknowledges the historical phases of AI in chemical engineering, noting that while AI's promise was not fully realized in the past, the current data science phase is ripe for success.

At the recent congress on Future Innovation in Process System Engineering (FIPSE), the focus was placed on the promising role of machine learning (ML) within process systems engineering (PSE). Its application is expected to revolutionize catalysis, enhance materials design, and improve process operations and automation [3]. There are numerous areas where machine learning techniques can be effectively utilized, including:

- Flowsheet analysis
- Surrogate modelling for simulation and optimization
- Integrated planning and scheduling
- Supply chain design and operation
- Process monitoring and fault diagnosis
- Real time optimization and control

The integration of symbolic causal reasoning reflected in the mathematical equations of core physical and chemical laws with data-driven methodologies is acknowledged as a major challenge and a significant opportunity for future development. The concluding report for the "AI Incubator Labs in the Process Industry," part of the EU project "Knowledge-Empowered Entrepreneurship Network" (KEEN), underscores the importance of combining actual process data, relevant domain knowledge, and AI methodologies during the entire life cycle of chemical plants. The primary goals include enhancing process efficiency, achieving economic advantages, and promoting sustainability. The project addresses three main AI application areas: (1) modelling and simulation of processes, products, and plants; (2) engineering of plants and processes; (3) optimal operation of production plants with the goal of self-optimizing plants [4]. A report from China highlights the significance of AI and robotic automation in chemical synthesis, particularly emphasizing its applications within the pharmaceutical industry. The primary focus is on the implementation of AI for the analysis of structure-function relationships, the strategic planning of synthetic routes, and the automation of the synthesis process [5]. AI support in mathematical chemistry resulted in the new field of digital chemistry and the revolutionary breakthrough in protein engineering. For many years, the complex problem of protein folding remained unresolved until DeepMind achieved a solution with atomic precision, leveraging structured deep neural networks to produce the AlphaFold open-access software tool. [6]. It will contribute to a rapid advancement in vital scientific and engineering disciplines. Another aspect of AI and digital chemistry is based on molecular descriptors. Each molecule can be projected in the space of about 6000 2D numerical descriptors applied for deep neural network processing. Industrially important cases are structural causal models of LPMO enzyme activity for biorefinery and textile waste water treatment, and prediction of deep eutectic properties for green separation processes [7-9]. Never-

theless, the majority of contemporary machine learning techniques rely on patterns derived from large datasets and statistical inference, which results in a lack of causal understanding. While they demonstrate strong predictive capabilities within the assumed static training framework, they fail to offer any mechanistic insights or causal explanations for their decision-making processes. Although this may not pose a significant issue in standard applications of computer vision, gaming, and recommendation systems, it holds considerable importance for various challenges in chemical engineering, including fault diagnosis, process control, and safety analysis. For chemical engineers key questions are on the second (effect of doing) and third rung (probability of counterfactual events) of Pearl's knowledge ladder [10-11]. The objective of this research is to outline the methodology for applying artificial intelligence in structural causal modeling (SCM) within the context of a chemical manufacturing plant, particularly the Tennessee Eastman (TE) challenge process.

2. Modelling

In chemical engineering, mass and energy balance models are typically represented as lumped, continuous, non-stationary, and deterministic systems characterized by ordinary non-linear differential equations (ODE):

$$\frac{dy}{dt} = f(y,x,\theta) \quad y(t=0)=y_0 \tag{1}$$

Bayes models are stochastic given by joint probability density function P

$$model = P(Y,X,\theta) \tag{2}$$

Dynamic Bayes on-line updated inference of the model variables $\{X,Y\}$ is based on prior and likelihood L of old evidence $\{Y_k, X_k\}\cdot$ Probability density distribution of the posteriori model is given by

$$\begin{pmatrix} Posteriori \\ model \end{pmatrix} = \begin{pmatrix} Likelhood \\ data \end{pmatrix} \cdot \begin{pmatrix} Prior \\ model \end{pmatrix} / \begin{pmatrix} Data \\ evidence \end{pmatrix} \tag{3}$$

$$P(\theta|Y,X) = \frac{P(Y,X|\theta)\cdot P(\theta)}{P(Y,X)} \tag{4}$$

Learning a Bayes network for a system model involves a two-step approach. The first step focuses on identifying the network structure G, which facilitates the factorization of the joint probability distribution P into separate local distributions P_i. In the second phase, parameters θ are estimated individually by either assuming a probabilistic framework or utilizing nonparametric inference methods such as neural networks or decision trees:

$$\begin{matrix} learning \\ P(G,\theta|data) \end{matrix} = \begin{matrix} structure \\ P(G|data) \end{matrix} \cdot \begin{matrix} parameter \\ P(\theta|G,data) \end{matrix} \tag{5}$$

The structure of the model, represented as $G=\{G_{knowledge}, G_{evidence}\}$, is defined as a directed acyclic graph (DAG). This graph consists of the model variables {Y,X}, which serve as nodes, and the arrows between them indicate direct causal relationships. In this research, $G_{knowledge}$ is derived from the connectivity of streams within the process sheet, along with an understanding of the mass and energy balance frameworks for each individual process unit. The unknown causal patterns $G_{evidence}$ are inferred from data by minimization of Bayes information criteria BIC. It is defined by likelihood L of data X, dimension of sampling space N, and model complexity (number of the graph parameters K).

$$BIC(X|G)=K\cdot ln(N)-2\cdot ln(L(X|G)) \tag{6}$$

Utilizing the hybrid heuristic hill climbing algorithm allows for effective reduction of the Bayesian Information Criterion (BIC) and supports the inference of the most likely graph G.

$$\hat{G} = \underbrace{min}_{i} [BIC(X|G_i)] \tag{7}$$

A causally decomposed process state space functions as a Markov system, facilitating a more straightforward inference of the joint probability density function P.

$$P(X) = \prod_{i=1}^{N} P(X_i|par(X_i)) \tag{8}$$

where $par(X_i)$ are the parent nodes which have a direct causal effect on X_i. To achieve process control objectives, it is essential to infer the causal effect on Y when the manipulative variable X is fixed deterministically at a value of x, as indicated by the "doing" function do $(X=x)$. Due to the present interaction between process variables, the evaluation of the effects of intervention requires d-separation of SCM graph. It produces an adjustment subset Z of process variables and offers a deconfounded "backdoor" estimation formula. [11]

$$\begin{aligned} P(Y|do(X)) &= \sum_{z\epsilon Z}^{Z} P(Y|X=x,\ Z=z)P(Z=z) \\ &= \mathrm{P(Y|W,\ Z)} \end{aligned} \tag{9}$$

The average treatment effect (ATE) quantifies the causal impact by measuring the average change resulting from the treatment.

$$ATE[y(x)] = \frac{d}{dx} E_Z[(Y|do(X)] \tag{10}$$

The expected value E_z associated with the covariates reflects the average causal effects calculated from the data within the adjusted control subset.

3. Process model

Causal AI modeling is utilized in the Tennessee Eastman plant-wide process, as proposed by Downs and Vogel (1993). This serves as a benchmark problem for various control-related topics, such as multivariable controller design, optimization, predictive control, estimation/adaptive control, nonlinear control, process diagnostics, and control education. This model represents the behavior of a standard industrial process, featuring a two-phase reac-

tor where an exothermic reaction takes place, in addition to a flash unit, a stripper, a compressor, and a mixer. The process exhibits a nonlinear and open-loop unstable behavior; in the absence of control, it can reach shutdown limits within an hour, even when subjected to minimal disturbances. The TE process, **Fig. 1**., produces two liquid products (*G* and *H*) and one (undesired) byproduct *F* from four gaseous reactants (*A*, *C*, *D* and *E*), according the reaction stoichiometry [12]

$$\begin{aligned} A + C + D &\rightarrow G \\ A + C + E &\rightarrow H \\ A + E &\rightarrow F \end{aligned} \qquad (11)$$

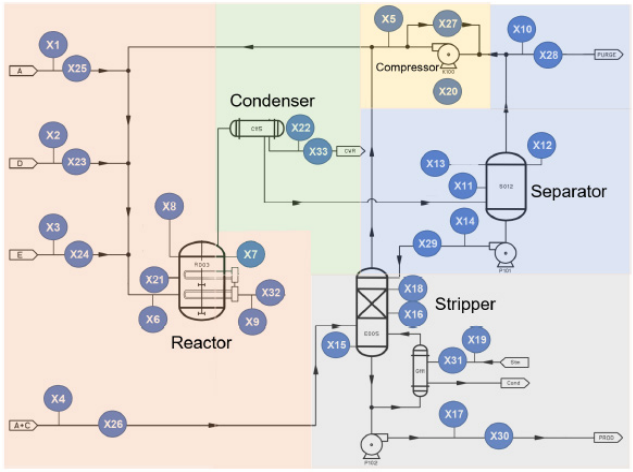

Fig. 1. Tennessee-Eastman process scheme [13-20]

Dynamic mass balances are given by the following ODE :

mixer

$$\frac{dN_{i,m}}{dt} = \sum_{j=1}^{6} y_{i,j} F_j - y_{i,6} \qquad i = A, \cdots H \qquad (12)$$

reactor

$$\frac{dN_{i,r}}{dt} = y_{i,6} F_6 - y_{i,7} F_7 + \sum_{j=1}^{3} v_{i,j} R_j \qquad i = A, .. H \qquad (13)$$

separator

$$\frac{dN_{i,s}}{dt} = y_{i,7} F_7 - y_{i,8} (F_8 + F_9) - x_{i,10} F_{10} \qquad i = A, .. H \qquad (14)$$

stripper

$$\frac{dN_{i,p}}{dt} = (1 - \phi_i)(x_{1,10} F_{10} + y_{i,4} F_4) - x_{i,11} F_{11} \qquad G, H \qquad (15)$$

Heat balances are given by:

mixer

$$\left(\sum_{i=A}^{H} N_{i,m} c_{p.vap,i}\right) \frac{dT_m}{dt} = \sum_{j=1}^{8} F_j \left(\sum_{i=A}^{H} y_{i,j} c_{p.vap,i}\right)(T_j - T_m) \qquad (16)$$

reactor

$$\left(\sum_{i=A}^{H} N_{i,r} c_{p.,i}\right) \frac{dT_r}{dt} = \mathrm{F}_6 \left(\sum_{j=A}^{H} y_{i,6} c_{p.vap,i}\right)(T_6 - T_r) - Q_r - \sum_{j=1}^{3} \Delta H_{rj} R_j \qquad (17)$$

separator

$$\left(\sum_{i=A}^{H} N_{i,s} c_{p.,i}\right) \frac{dT_s}{dt} = \mathrm{F}_7 \left(\sum_{i=A}^{H} y_{i,7} c_{p.vap,i}\right)(T_r - T_s) - Q_s - H_0 V_s \qquad (18)$$

striper

$$\begin{aligned} \left(\sum_{i=G}^{H} N_{i,p} c_{p.,i}\right) \frac{dT_p}{dt} = \mathrm{F}_{10} \left(\sum_{i=A}^{H} x_{i,10} c_{p.,i}\right)(T_s - T_p) + \\ + F_4 \left(\sum_{i=A}^{H} y_{i,4} c_{p.vap,i}\right)(T_4 - T_p) - H_0 V_p + Q_p \end{aligned} \qquad (19)$$

The system is a lumped MIMO DAE model consisting of 30 nonlinear state *y* differential ordinary differential equations (ODEs) and 149 algebraic equations *x*, incorporating 10 input variables and 130 physical and chemical parameters θ. Simulation software is included within the MatLab Simulink software support framework [18]. The results of these simulations can be accessed through Harvard Dataverse and GitHub repositories [17,20].

4. Results and discussion

The analysis utilizes a dataset comprising 50,000 randomly selected samples of process variables, collected under normal operating conditions during a simulated 48-hour continuous operation. The data includes 12 manipulative control variables (exogenous) and 35 continuous variables (endogenous), as illustrated in Fig. 1 [19]. The data exhibit a Pearson correlation coefficient of R=0.22, indicating a moderate level of correlation. The focus of the analysis is on predicting and understanding the causal effects of process variables on the production rates of G and H. For numerical and statistical evaluation the R language and "q*eML*" machine learning tool wrapper are applied [21-23].

The "random forest" algorithm was utilized to assess the significance of variables by measuring the improvement in the predictive accuracy of G product's productivity. The results of the variable relative importance are depicted in **Fig. 2**. The reactor pressure, separator temperature, and stripper pressure account for approximately 95% of the overall significance in predicting G productivity. Because of the confounding effects introduced by multivariate correlation, the importance factors identified do not reflect the direct causal relationships of the variables with G production. Utilizing a complete set of 34 predictor variables, the "random forest" machine learning model has shown impressive predictive accuracy, as evidenced by tests conducted on 8,000 trained samples and 2,000 untrained samples, **Fig. 3**. The model successfully accounts for 95% of the data variance, with mean relative absolute errors of 1.9% for the trained data and 2.2% for the untrained data related to G production.

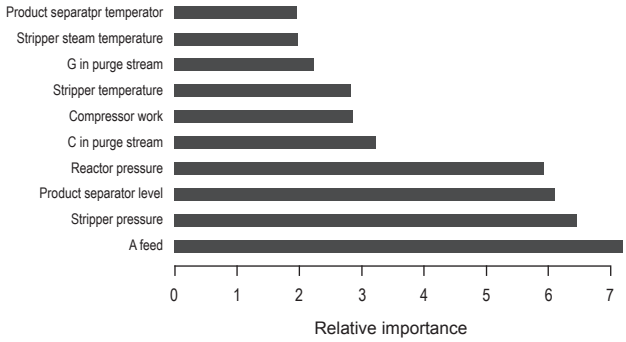

Fig. 2, Variable importance for the ML model prediction of *G* production.

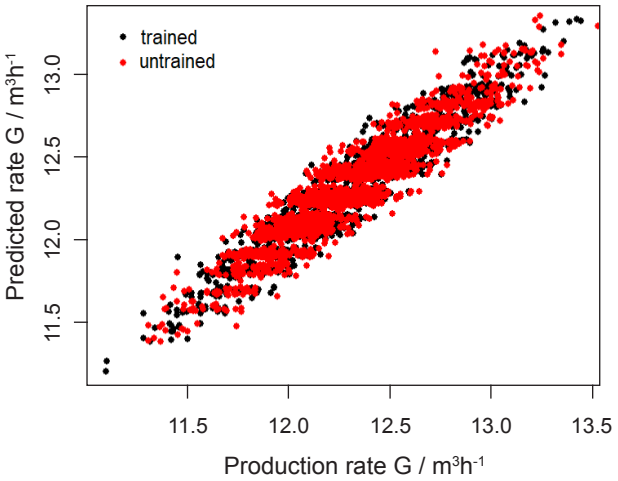

Fig. 3. Comparison of the random forest model (RF) predictions and values of G purge rate.

While the RF model demonstrates a high level of prediction accuracy, its agnostic nature—implying a presumed absence of domain knowledge—renders it unsuitable for do*(X=x)* analysis of causal relationships. This analysis is crucial for making informed decisions regarding process interventions, control policies, and optimization strategies.

The studied TE serves as a model for a manufacturing production system, grounded in the principles of chemical engineering, resulting in highly detailed and precise field knowledge (eq. 12-19). Deterministic direct causal relationships are established through functional forms of mass and energy balances, stoichiometric relationships of chemical reactions, and causal connections derived from the design of process synthesis, as represented in a process sheet or graph. In practice, certain process parameters are estimated with inherent uncertainties, while others remain unknown, particularly kinetic parameters. Additionally, some interactions may be unforeseen, such as catalyst poisoning, and there are process disturbances that go unobserved. The Bayes network AI model is proposed which accounts for causal effects of stochastic nature present in an industrial process. The known structural causality, given as graph $G_{knowledge}$, is integrated with data inferred causality G_{data}.

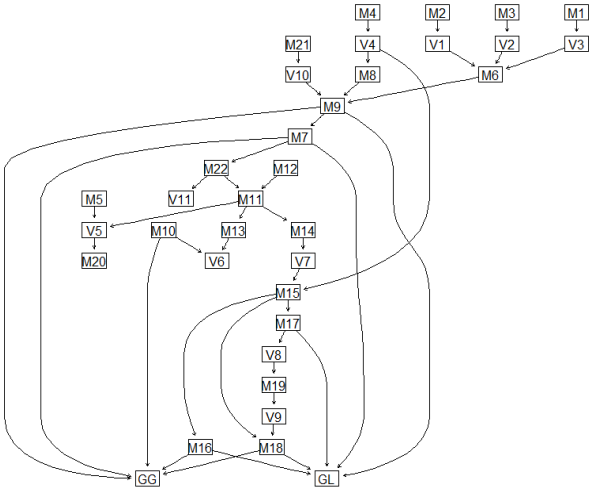

Fig. 4. Directed acyclic graph (DAG) of TE process. M are measured state variables, manipulative variables V, product G in liquid and gas purge are GL and GL M9 and M7 are reactor temperature and pressure.

Table 1. Labels of the process flow sheet

M1	A feed (stream 1)
M2	D feed (stream 2)
M3	E feed (stream 3)
M4	A and C feed (stream 4)
M5	recycle flow (stream 8)
M6	reactor feed rate (stream 6)
M7	reactor pressure
M8	teactor level
M9	reactor temperature
M10	purge rate (stream 9)
M11	product separator emperature
M12	product separator level
M13	product separator pressure
M14	product separator underflow (stream 10)
M15	stripper level
M16	stripper pressure
M17	stripper underflow (stream 11)
M18	stripper temperature
M19	stripper steam flow
M20	compressor work
M21	reactor cooling water outlet temperature
M22	separator cooling water outlet temperature
V1	D feed flow (stream 2)
V2	E feed flow (stream 3)
V3	A feed flow (stream 1)
V4	A and C feed flow (stream 4)
V5	compressor recycle valve
V6	purge valve (stream 9)
V7	separator pot liquid flow (stream 10)
V8	stripper liquid product flow (stream 11)
V9	stripper steam valve
V10	reactor cooling water flow
V11	condenser cooling water flow

Table 2. Canonical adjusted sets of the control variables for product G_{liquid} and Markov blankets of the reactor variables.

Adjusted control variables for product G_{liquid}	
M9: reactor temperature	M1, M12, M2, M21, M3, M4, M6, M8, V1, V10, V2, V3, V4
M7: reactor pressure	M1, M12, M2, M21, M3, M4, M6, M8, M9, V1, V10, V2, V3, V4
Markov blankets for the reactor	
M9: reactor temperature	M10, M16, M17, M18, M6, M7, M8, V10, GG, GL
M7: reactor pressure	M10, M16, M17, M18, M22, M9, GG, GL

Integrated structure $G = \{G_{knowlrdge}, G_{data}\}$, N observed data, and K number of the model parameters are jointly evaluated by minimization of the corresponding Bayes information criteria, BIC, eq. 6. Applied is hybrid heuristic MMHC algorithm [25-26]. To identify the G skeleton, MMHC employs tests of conditional independence, seeking variable subsets Z that render a pair of variables X and Y conditionally independent. They are inferred from the corresponding conditional independence as proposed in the stable PC algorithm [26]. The application of heuristic local optimization in the G search space results in the most probable posterior Bayes network model, leveraging known prior causal structure and causal relationships inferred from the data observed (eq. 7). The obtained model is the DAG graph presented in **Fig. 4**. The model accounts for the measured state variables (M), manipulative variables (V), and production rate of product G in gas purge stream and liquid striper underflow (GG, GL). The structure of the DAG model achieved allows for d-separation, effectively preventing "back door" confounding of causal effects. The adjusted sets Z of control variables, which account for the dependence of GL on reactor temperature and pressure, are presented in Table 2. The corresponding Markov blanket sets yield the paternal, children, and children parent nodes by which the reactor temperature and pressure are separated from the perturbations of the rest of process variables. Pair-wise causal dependencies are depicted in **Fig. 5**. The graphs shown represent partial dependency plots generated by Bayes neural networks, which were trained on the relevant adjusted Z sets. The method applies single inner layer network configurations featuring sigmoid activations, with backpropagation used for the learning mechanism. The graphs are traces of individual $Y[\mathrm{do}(x)]$ where Y is the molar percentage of the product G in the separator underflow liquid stream, and x are the following process variables: compressor recycle % opening, E feed stream, input mixed A and C stream, and D feed rate. The developed model facilitates the estimation of indirect causal relationships that remain obscured due to implicit nonlinearities, making them not readily apparent from prior structural knowledge. The observed dispersions of the causal plots are due to the effects of variability of the rest of variables from the corresponding adjusted control sets. Bivariate effects of synergism and antagonism are depicted in Fig. 6. The plots are two-dimensional partial dependency plots of the estimated expected values Ez[Y(x1,x2)] where x1 and x2 are selected variables from the adjusted control set of Y and averaging E covers the complimentary set Z/(x1,x2). The f results facilitate the visualization of causal synergism within a system characterized by opaque and intricate nonlinear interactions.

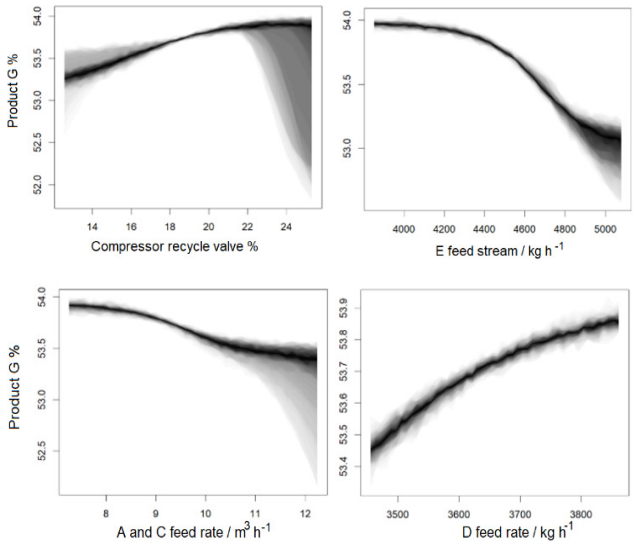

Fig. 5. Bayes NN predictions of causal dependances of the production rate of G in liquid outlet

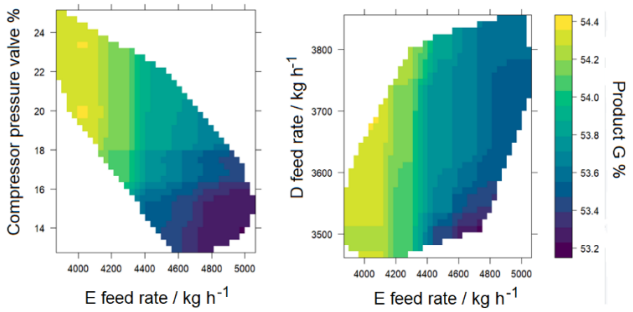

Fig. 6. Bayes NN bivariate causal partial plots of the dependency of molar G% in liquid outlet stream on the key process variables.

The visualization of causal interactions provides basis for design of multilevel control system, process optimization, and synthesis of alarm system for fault detection.

5. Conclusions

The causal artificial intelligence model offers engineers insights into the impacts of decisions and interventions within a manufacturing system, particularly under novel and previously unobserved conditions. Formally, it infers numerical functions of ATE (average treatment effect, doing $Y[\mathrm{do}(X{=}x)]$) and/or CATE (conditioned average treatment effect, doing $Y[\mathrm{do}(X{=}x)|Z{=}z)]$) effectsThe improvement of agnostic machine learning models is of utmost importance, given that their regressive property limits their ability to make predictions solely based on conditions that have been previously encountered. The modeling of causality utilizes Bayesian networks, which facilitate an advanced level of artificial intelligence and enable causal inferences that

align with the second tier of Pearl's knowledge ladder[11]. The primary characteristic of causal Bayes networks is their structural representation of direct causal relationships, which adhere to the Markovian property.

In the context of industrial systems, structural knowledge is largely grounded in causal structural equations that originate from basic principles of mass and energy conservation, as well as the schematics of designed process flows. It is possible to infer unobserved or unknown interactions by merging a priori structural insights with statistical conditional analysis or by optimizing the Bayesian Information Criterion (BIC) in the context of causal networks. The representation of system structural knowledge takes the form of a directed acyclic graph (DAG) that includes process variables, with network nodes linked by direct causal connections indicated by arrows. DAG networks exhibit Markovian properties, allowing the joint probability function to be decomposed into the products of the probability distributions of simple parent nodes. Unknown physical and chemical parameters are incorporated within the node regression parameters and/or weights of neural networks, utilizing substantial data collected from process monitoring..

The methodology and analysis of causal artificial modeling are utilized in the examination of the chemical synthesis process at the Tennessee Estman industrial complex. The process in question is a catalytic, two-phase (gas and liquid) system that exhibits instability. Initial structural understanding is obtained through basic mass and energy balance calculations, as well as the relationships between mass and heat streams specified in the process flow sheet. Unobserved causal relationships can be effectively identified through the heuristic minimization of the Bayesian Information Criterion (BIC) within the model. This causal model provides unconfounded estimates regarding the importance of process variables, utilizing adjustment sets as control variables. It also incorporates the Markov blankets for reactor pressure and temperature, along with average treatment effects (ATE) and the synergistic interactions between process variables.

Causal AI models offer vital information that is crucial for the optimization of processes, the innovation of operational methods, the development of intelligent control systems, and the support of decision-making strategies in manufacturing [27].

From a chemical process engineering standpoint, the main difference in the applicability of causal Bayes networks versus first principle models, like mass and energy balances, is their consideration of stochastic effects. Causal Bayes networks effectively address both exogenous variables (process feeds) and endogenous variables (generated by the process), particularly in terms of kinetics and mass/energy transfer coefficients. In summary, fundamental mathematical models serve as the foundation for process design, whereas Bayes causal AI models concentrate on process control and decision-making policies for interventions in uncertain environments.

6. References

[1] URL: https://research-and-innovation.ec.europa.eu/ research-area/industrial-research-and-innovation/ industry-50_en

[2] Venkatasubramanian V., The promise of artificial intelligence in chemical engineering, AIChE Journal 65 (2019) 466-478

[3] Daoutidis P., Lee J.H., Rangarajan S., Chiang L., Gopalani B., Schweidtmann A., Harjunkoski I., Mercangoz M., Mesbah A., Boukouvala F., Limo F.V., Chanona A., Georgakis C., Machine learning in process systems engineering: Challenges and opportunities, Comput Chem Eng, 181 (2024) 108523

[4] Bortz M., Dadhe K., Engell S., Gepert V., Kockmann N., Muller Pfefferkon R., Schindler T., Urbas L, AI in Process Industries – Current Status and Future Prospects Chem Eng Tech 95 (2023) 975-988

[5] He, C., Zhang, C., Bian, T., Jiao, K., Su,W., Wu, K, Su, A. A Review on Artificial Intelligence Enabled Design, Synthesis, and Process Optimization of Chemical Products for Industry 4.0. Processes 11 (2023) 330

[6] Jumper J., Evans R., Pritzel A., Green T, Figurnov M., Ronneberger O., Tunyasuvunakool K., Bates R., Žídek A., Potapenko A., Bridgland A., Meyer C., Kohl S., Ballard A., Cowie A., Romera-Paredes B., Nikolov S., Adler J., Back T., Petersen S., Reiman D., Clancy E., Zielinski M., Steinegger M., Pacholska M., Berghammer T., Bodenstein S., Silver D., Vinyals O., Senior A.W., Kavukcuoglu K., Kohli P., Hassabis D., Highly accurate protein structure prediction with AlphaFold, Nature 596 (2021) 583.

[7] Rezić, I., Kracher, D., Oros, D., Mujadžić, S., Anđelini, M., Kurtanjek, Ž., Ludwig, R., Rezić, T., Application of Causality Modelling for Prediction of Molecular Properties for Textile Dyes Degradation by LPMO, Molecules,19 (2022), 1-13

[8] Rezić T., Vrsalović Presečki A., Kurtanjek Ž., New approach to the evaluation of lignocellulose derived by-products impact on lytic-polysaccharide monooxygenase activity by using molecular descriptor structural causality model, Bioresour Technol, 342 (2021) 125990

[9] Kurtanjek Ž., Molecule Structure Causal Modelling (SCM) of Choline Chloride Based Eutectic Solvents, Chem Biochem Eng Q 36 (2022) 223–230

[10] Efron B., Hastie T., Computer Age Statistical Inference – Algorithms, Evidence, and Data Science, Cambridge University Press, New York. 2016

[11] Pearl J., Mackenzie D., The Book of Why: The New Science of Cause and Effect, Penguin Books, Harlow, 2019, UK

[12] Downs, J.J., and Vogel, E.F. A Plant Wide Industrial Process Control Problem, Comput. Chem. Eng., 17 (1993) 245–255.

[13] Jockenhövel T., Biegler L.T., Wächter A., Comput. Chem. Eng., 27 (2003), 1513-1531.

[14] Sales-Cruz, M., Cameron, I., & Gani, R. Tennessee Eastman Plant-wide Industrial Process Challenge Problem. In I. Cameron, & R. Gani (Eds.), *Product and Process Modelling: A Case Study Approach* 9 (2011) 273-303.

[15] Ricker, L.N. Tennessee Eastman Challenge Archive, http://depts.washington.edu/ctrol/LARRY/TE/download.html#Decentralized_control (2005)

[16] Capaci, F., Vanhatalo, E., Kulahci, M., & Bergquist, B. The revised Tennessee Eastman process simulator as testbed for SPC and DoE methods. Qual. Eng., 31 (2019) 212-229

[17] R. Braatz, https://github.com/camaramm/tennessee-eastman-profBraatz (2023)

[18] Jenny, O.E., MATLAB Central File Exchange. TE process (https://www.mathworks.com/matlabcentral/file exchange/39742-te-process), 2023.

[19] Menegozzo, G., Dall'Alba, D., & Fiorini, P. CIPCaD-Bench: Continuous Industrial Process datasets for benchmarking Causal Discovery methods. 2022 IEEE 18th International Conference on Automation Science and Engineering (CASE), (2022). 2124-2131.

[20] Cory R, A., Amsel, B. D., Randy T.,; Cook, M. B., "Additional Tennessee Eastman Process Simulation Data for Anomaly Detection Evaluation", Harvard Dataverse, V1 https://doi.org/10.7910/DVN/6C3JR1, (2017),

[21] R Core Team R: A language and environment for statistical computing. R Foundation for Statistical Computing, Vienna, Austria. URL https://www.R-project.org/ (2023).

[22] RStudio Team RStudio: Integrated Development for R. PBC, Boston, MA URL http://www. rstudio.com/ (2020)

[23] Matloff N., qeML, https://github.com/matloff/qeM (2023)

[24] Kurtanjek Ž., Kada zaključivanje matematičkim modelom može biti pogrešno: Primjer protočnog kemijskog reaktora PKR, Kem. Ind. 70 (2021) 739–741

[25] Tsamardinos, I., Brown L.E., Aliferis C.F., The max-min hill-climbing Bayesian network structure learning algorithm, Mach Learn 65 (2006) 31–78

[26] Scutari M. Learning Bayesian Networks with the bnlean R Package. J. Stat. Softw., 35 (2010), 1-22URL http://www.jstatsoft.org/v35/i03/

[27] Pu H., Chen Z., Liu J., Yang X., Ren C., Liu H., Yian Y., Research on decision-level fusion method based on structural causal model in system-level fault detection and diagnosis, Eng. Appl. Artif. Intell., 126 (2023) 107095